THE UNIVERSITY OF MICHIGAN RESEARCH INSTITUTE
ANN ARBOR

STUDY OF INPUT CIRCUITRY OF DIRECTION FINDER SET AN/TRD-4A

Technical Memorandum No. 77

Cooley Electronics Laboratory
Department of Electrical Engineering

By: C. E. Lindahl

Approved by: H. W. Farris

H. W. Farris

Project 2899

TASK ORDER NO. EDG-10
CONTRACT NO. DA-36-039 sc-78283
SIGNAL CORPS, DEPARTMENT OF THE ARMY
DEPARTMENT OF ARMY PROJECT NO. 3A99-06-001-01

July 1960

TABLE OF CONTENTS

LIST OF ILLUSTRATIONS

LIST OF TABLES

ABSTRACT

A study is made of the input circuitry of the radio direction finder set AN/TRD-4A. This circuitry consists of the antennas, the antenna connecting cables, the goniometers, and the transmission line-RF switch combination connecting the signal goniometer to the receiver.

One objective of this study is to determine the effect of each component of the input system on the power finally delivered to the input impedance of the receiver; hence, transmission loss calculations based upon experimental measurements were made for each of the components.

In conclusion it can be said that the overall transmission loss could be decreased significantly by matching impedance levels throughout the system.

STUDY OF INPUT CIRCUITRY OF DIRECTION FINDER SET AN/TRD-4A

1. INTRODUCTION

A study was initiated concerning the input circuitry of the AN/TRD-4A direction finder, namely, the antennas, the antenna connecting cables, the goniometers, and the transmission line-RF switch combination connecting the signal goniometer to the receiver. The reasons for this study were twofold: 1) to become familiar with the AN/TRD-4A operating as a direction finder; and 2) to study those components which are critical factors in determining the equipment sensitivity. The methods used in the study and the results obtained follow.

One of the objectives of this study was to determine the effect of each component of the input system on the power finally delivered to the input impedance of the receiver.

2. DESCRIPTION OF THE INPUT SYSTEM

Figure 1 shows a block diagram of all the components of the input system of the TRD-4.

The Adcock antenna system consists of two vertically-polarized U Adcock antennas placed as shown in Fig. 2. Each U Adcock antenna consists of two monopoles erected over a counterpoise used to establish a satisfactory ground plane. The spacing between the monopoles and their heights depend upon the frequency band to be covered. The low-frequency band covers from 0.5 mc to 10.0 mc; the high, from 8 mc to 30 mc. The

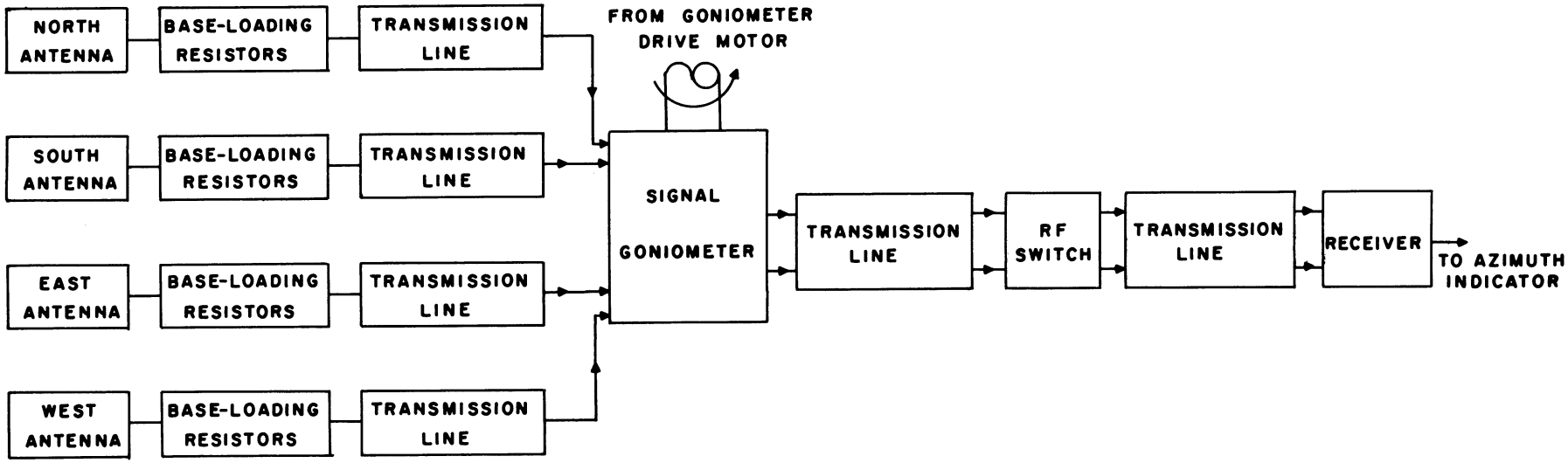

FIG. 1 BLOCK DIAGRAM OF INPUT CIRCUITRY

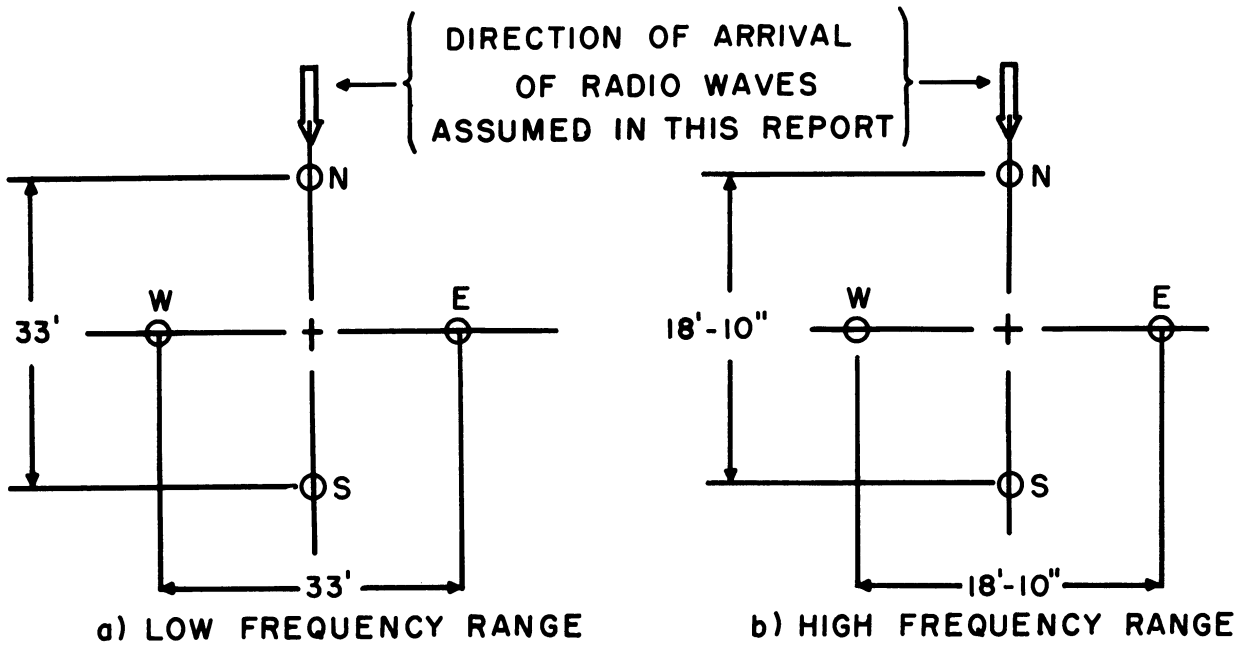

FIG. 2 PLAN VIEW OF ANTENNA CONFIGURATION FOR LOW (0.5MC TO 10MC) AND HIGH (8MC TO 30MC) FREQUENCY RANGES

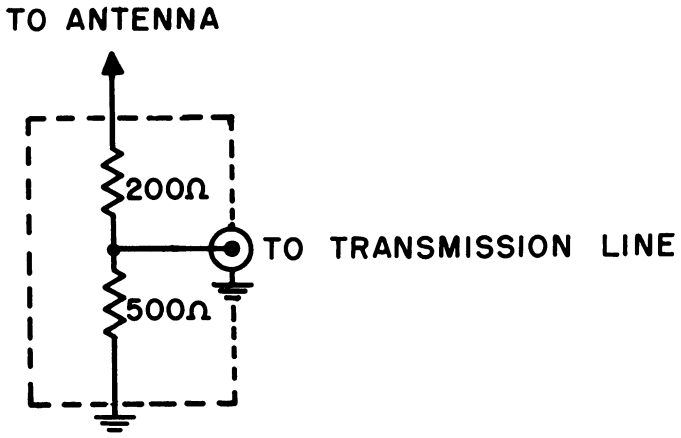

FIG. 3 BASE-LOADING RESISTOR DIAGRAM

required spacings of the antennas for these bands are shown in Fig. 2. The height of each monopole used in the low range (0.5-10.0 mc) is 29 feet with an antenna top-loading disk on each. In the high range (8-30 mc) a height of 22'-4" is used.

The base-loading resistors are located in an antenna coupler unit fastened to the base of each monopole. The circuit diagram is shown in Fig. 3. It is understood that the purpose of these resistors is to damp-out antenna resonances which cause bearing errors.

The matched transmission lines connecting each monopole to the signal goniometer consist of 170 feet of RG-13A/U coaxial cable.

Two types of signal goniometers are used. The type GO-5/GRD electrical goniometer is used in the frequency range from 0.5 mc to 10 mc; the GO-6/GRD, from 8 mc to 30 mc. Figures 4 and 5 show the circuit diagrams of these devices. The purpose of these signal goniometers is to combine the signals from the antennas in such a way that the output consists of only two side bands with the carrier signal suppressed. After the resultant goniometer output is passed through the receiver of the direction finder and the signal is demodulated in the azimuth indicator, the bearing of the incoming wave can be determined.

The transmission lines connecting the goniometer to the RF switch and, in turn, the RF switch to the receiver, consist, respectively, of 2-foot and 3-foot-5-inch pieces of RG-22B/U coaxial cable.

The RF switch is used to switch from a signal goniometer mode to a single-loop operating mode and vice versa. Figure 6 shows its circuit diagram when switched to the goniometer operating mode.

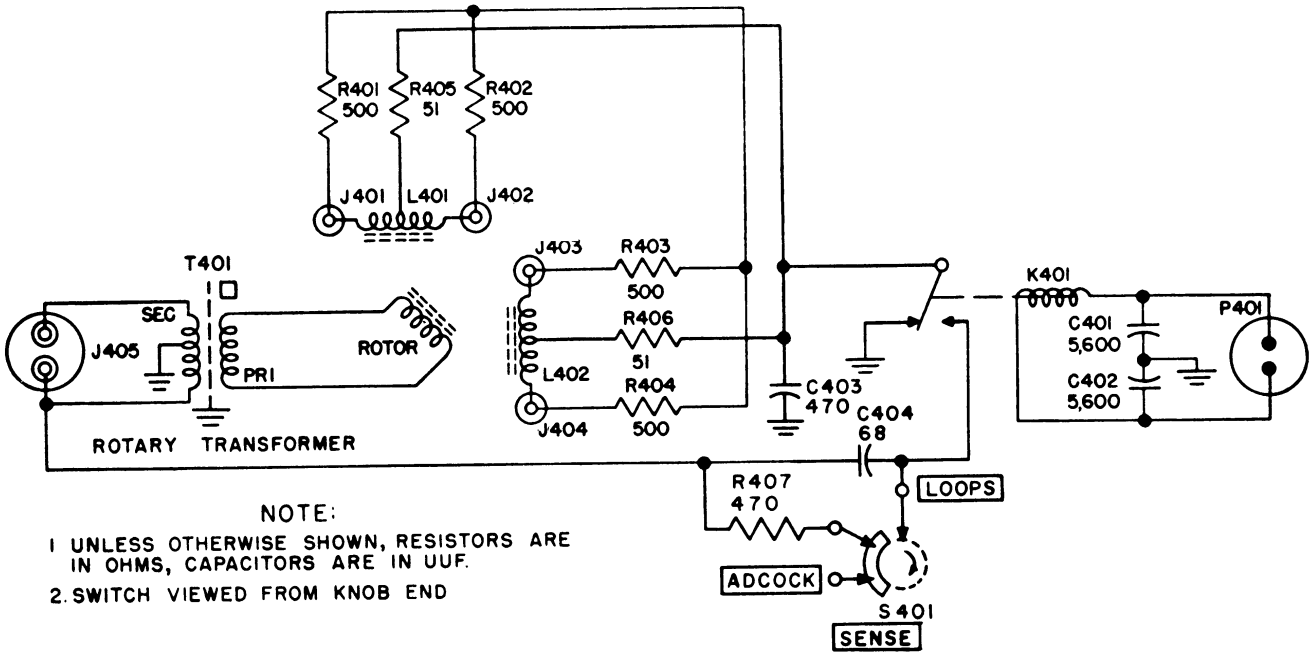

FIG.4 ELECTRICAL GONIOMETER GO-5/GRD

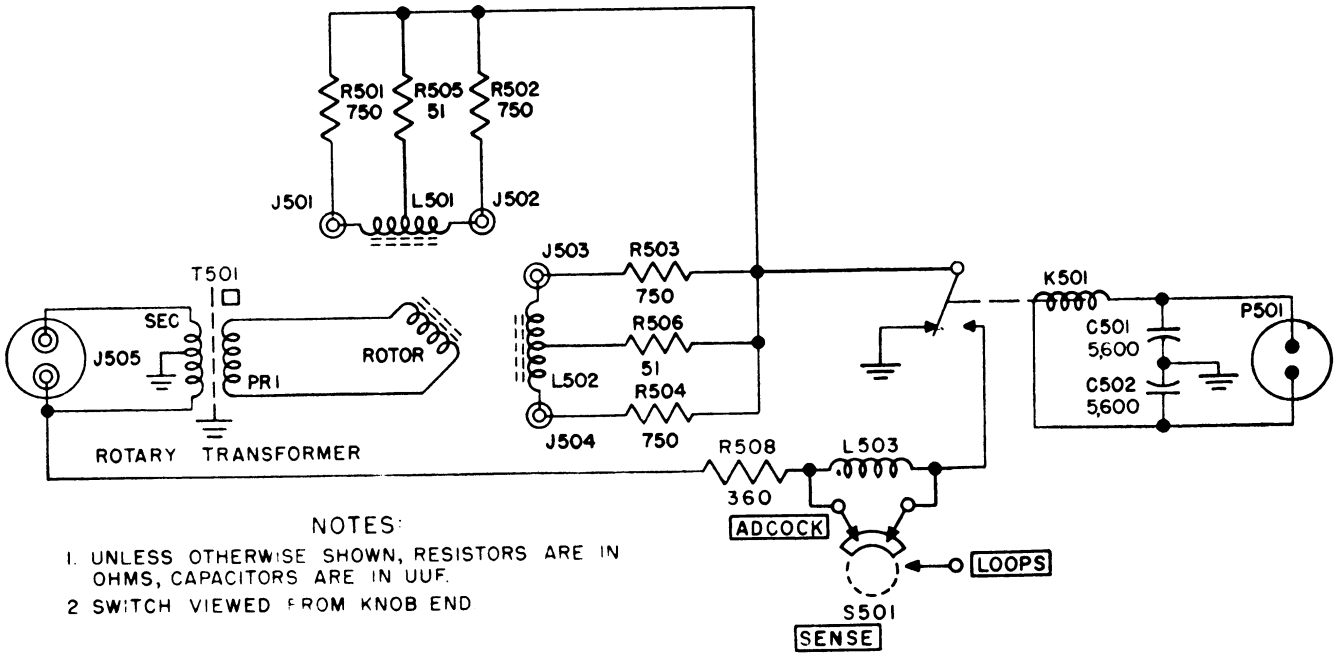

FIG.5 ELECTRICAL GONIOMETER GO-6/GRD

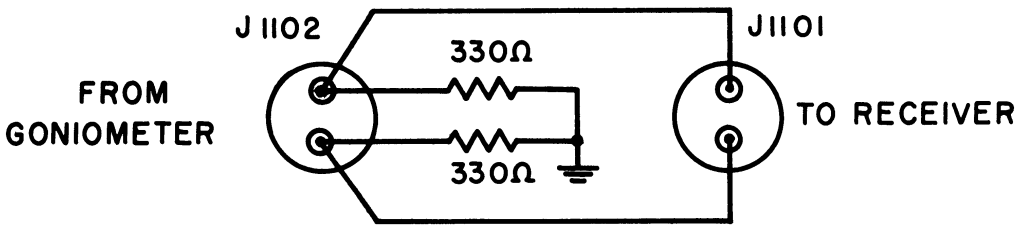

FIG. 6 CIRCUIT DIAGRAM OF RF SWITCH IN GONIOMETER OPERATING POSITION.

3. ADCOCK ANTENNAS

The impedances of both the low- and high-frequency antennas were measured, and the results are shown on the Smith charts of Figs. 7, 8, and 9. Since the base-loading resistors are connected physically to each monopole, an impedance measurement was taken with and without the loading resistors connected. All impedances were normalized to 74 ohms, the characteristic impedance of the RG-13A/U connecting cables.

An equivalent circuit of a linear antenna can be derived by Thévenin's theorem. Such an equivalent is shown in Fig. 10, where Z_a equals the antenna impedance as measured above and $\underline{V}$ equals the open-circuit voltage across the antenna terminals when an electromagnetic wave impinges on the antenna. In order to relate the voltage, $\underline{V}$, to the electromagnetic wave, we can define the effective height, $\underline{h}$, of the antenna which equals the ratio of this voltage, $\underline{V}$, to the magnitude of the electric field intensity, $\underline{E}$, where V is in volts and E is in volts/meter. It is

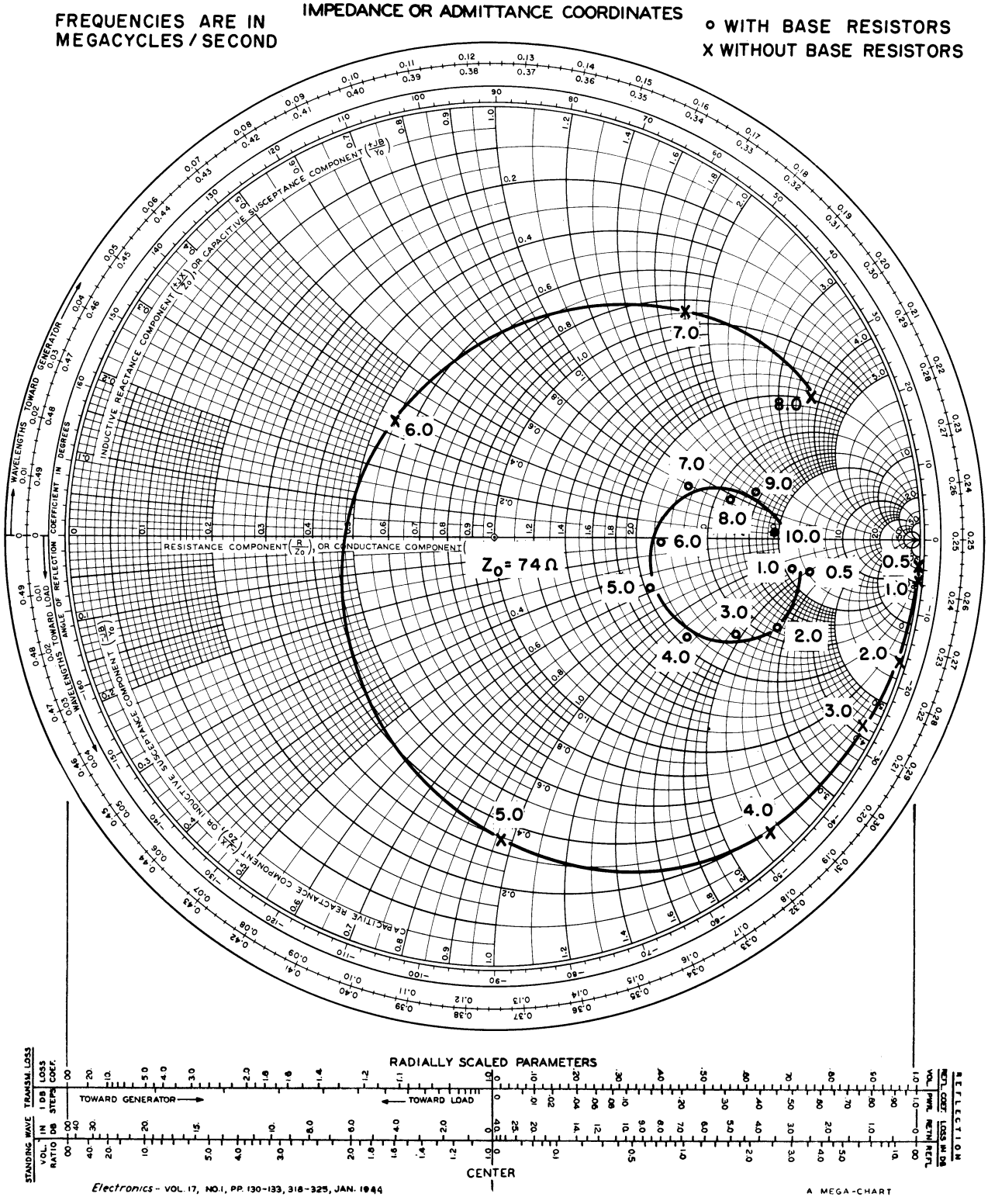

FIG. 7 INPUT IMPEDANCE OF AN/TRD-4A LOW FREQUENCY ANTENNA.

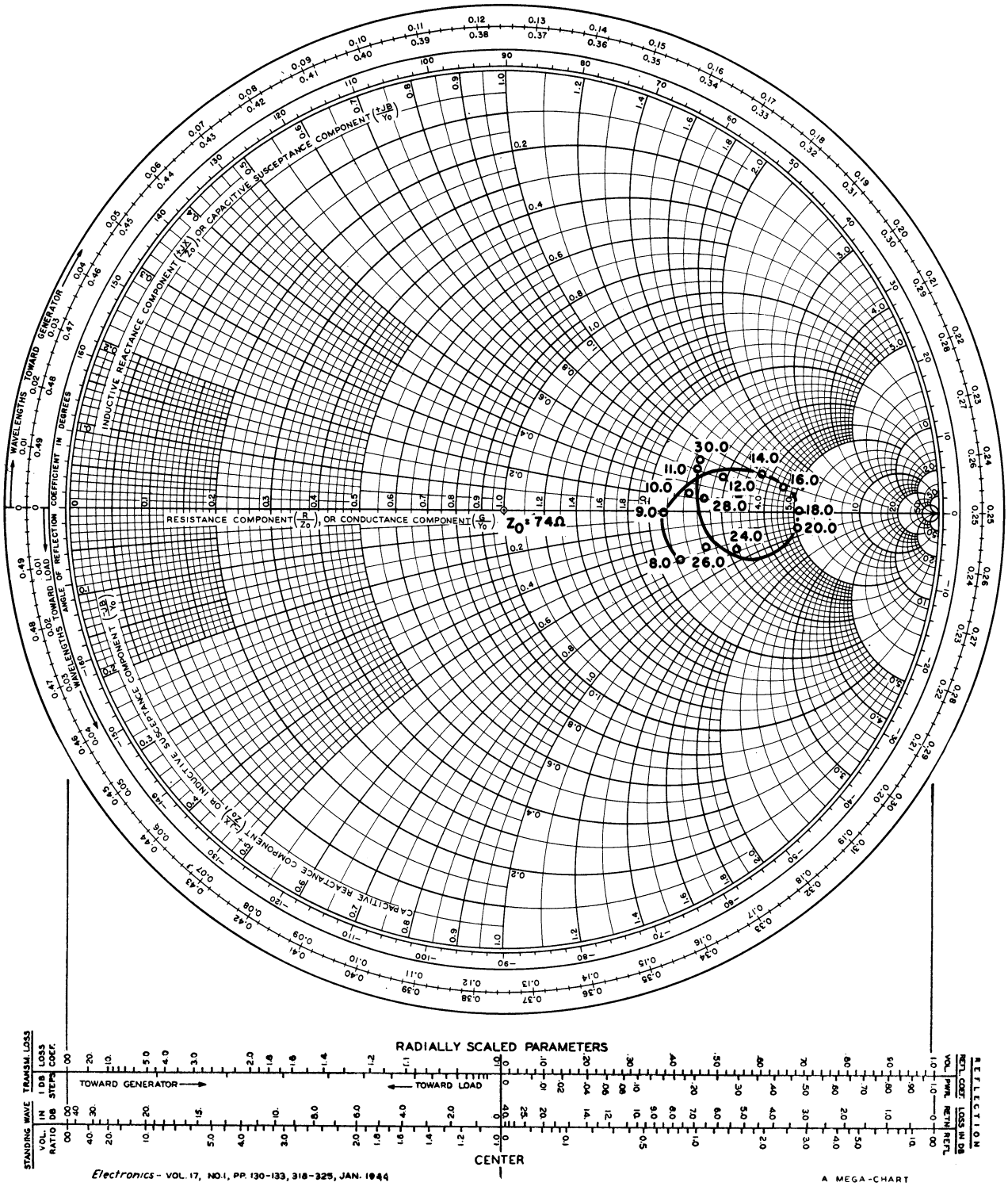

FREQUENCIES ARE IN MEGACYCLES / SECOND

FIG.8 INPUT IMPEDANCE OF AN/TRD-4A HIGH FREQUENCY ANTENNA WITH BASE RESISTORS.

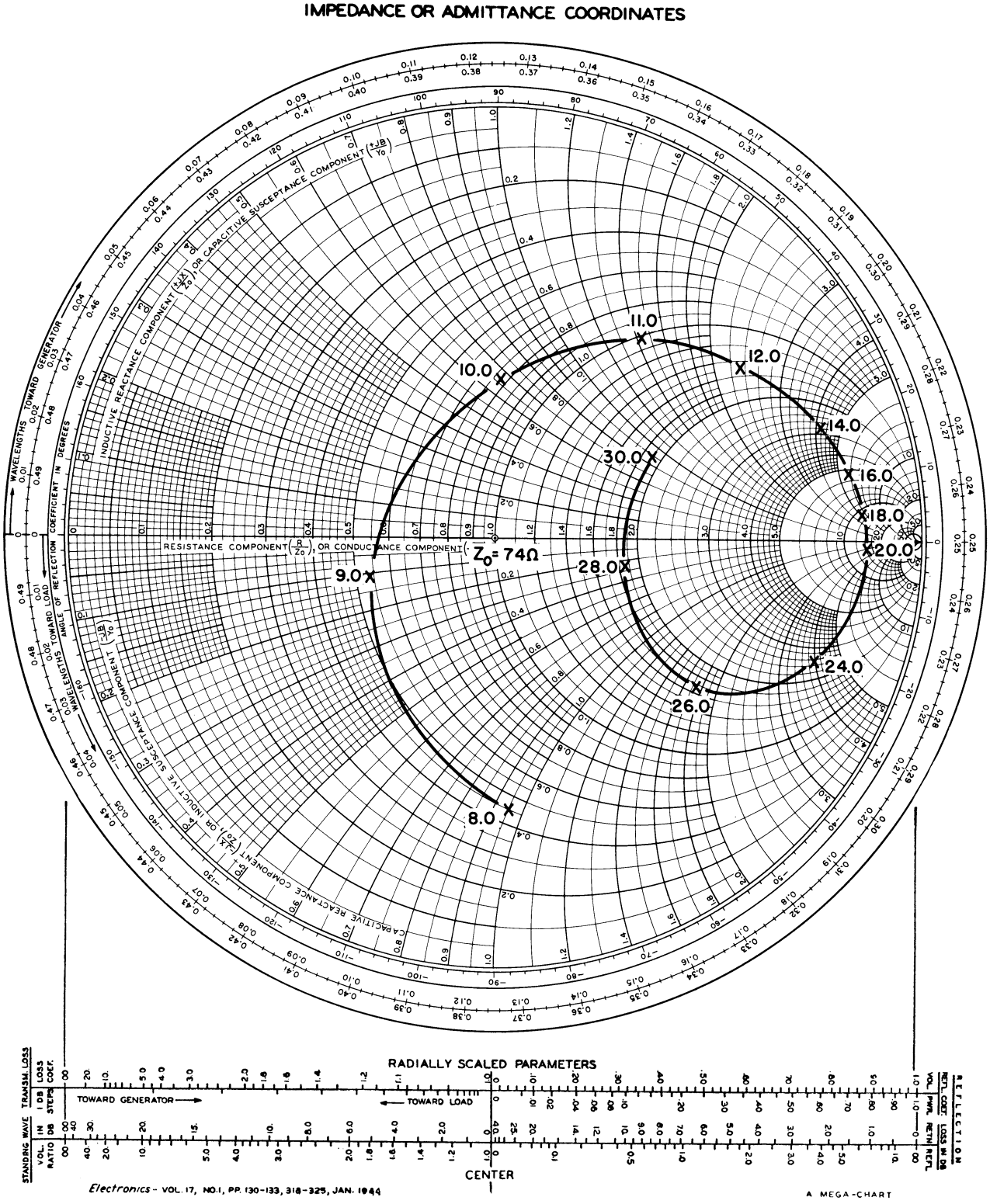

FREQUENCIES ARE IN MEGACYCLES / SECOND

FIG. 9 INPUT IMPEDANCE OF AN / TRD-4A HIGH FREQUENCY ANTENNA WITHOUT BASE RESISTORS.

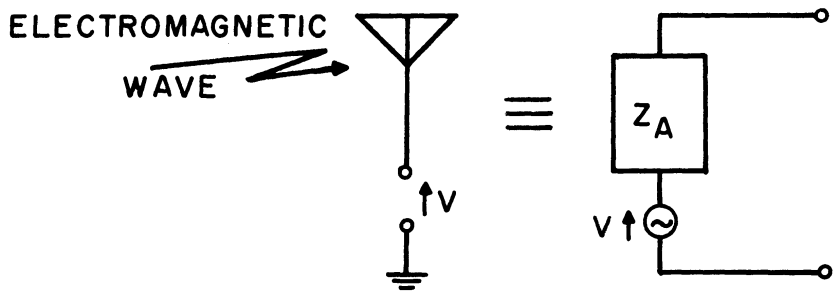

FIG. 10 THEVENIN EQUIVALENT OF A LINEAR ANTENNA.

assumed that $\underline{E}$ is vertically polarized. The best way to determine the effective height is to measure it experimentally if suitable field-strength measuring equipment is available. However, this not being the case, this report treats only the input system components following the antennas.

4. MEASUREMENT METHODS AND CALCULATION PROCEDURES

The results stated were all obtained by the measurement of various impedances. From these pertinent impedance values, calculation procedures were used to obtain the desired result. As stated above, one of the objectives was to determine the effect of each component of the input system on the power finally delivered to the receiver input impedance. In order to do this, certain assumptions had to be made. These were: 1) all components are linear within their normal operating ranges; 2) the transmission lines between the base-loading resistors and the signal goniometer are selected so that their electrical characteristics are identical, as are the base-loading resistors themselves; 3) the monopole antennas are identical; 4) the base-loading resistors are resistive throughout the

frequency range used; 5) the north-south, east-west, and output terminals of the signal goniometer are balanced with respect to ground; 6) the transmission line-RF switch combination between the goniometer and the receiver is balanced with respect to ground; and finally 7) the receiver input is balanced with respect to ground. The above assumptions were verified within the experimental accuracy of the measuring equipment used.

The input system can be divided into two parts, the north-south system and the east-west system. Throughout all the measurements it was assumed that a signal was arriving from the north as shown in Fig. 2. The signal goniometer rotor was locked in such a position that its output would be maximum when a wave arrived from the assumed azimuth angle. Under these conditions the voltage developed at the goniometer output by the east-west U Adcock is zero; hence, we need consider only the north-south antenna system. Since the east-west and the north-south systems are identical, analysis of only one of them is necessary to determine the system behavior. The system analyzed is shown in Fig. 11.

In order to determine how power is transmitted from the output of the antennas to the input impedance of the receiver, one must first know how each component of the system alters this power transfer. One way of doing this is to measure experimentally the open- and short-circuit impedances of the components and then from these measurements calculate the A, B, C, D parameters of each component part. The A, B, C, D parameters are defined by the following equations describing the behavior of the linear, passive, bilateral network shown in Fig. 12.

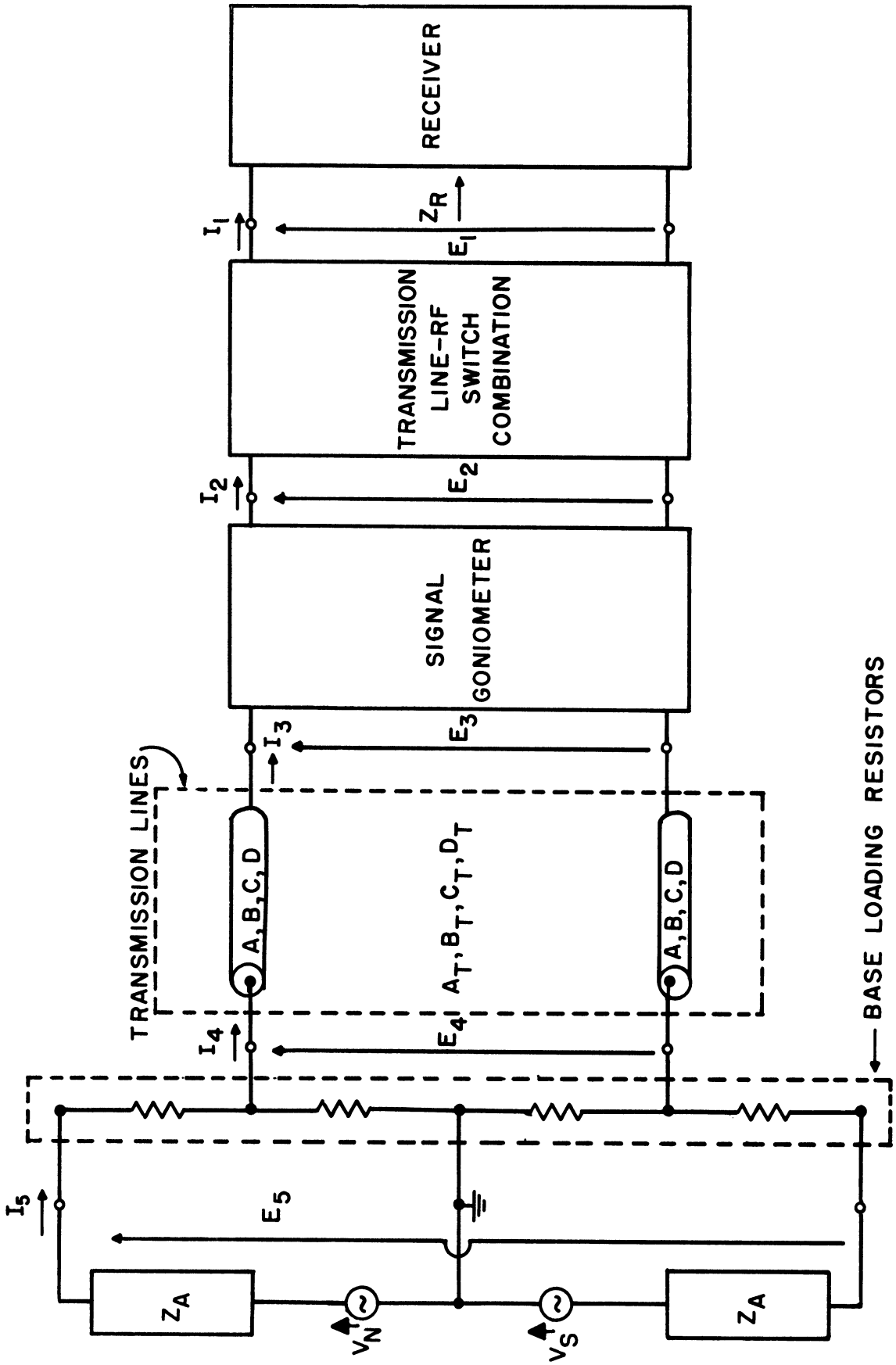

FIG. 11 BLOCK DIAGRAM OF NORTH-SOUTH INPUT SYSTEM.

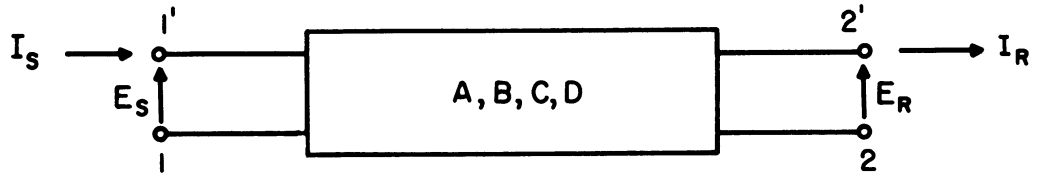

FIG. 12 LINEAR, PASSIVE, BILATERAL NETWORK.

$$E_S = AE_R + BI_R \tag{1}$$

$$I_S = CE_R + DI_R \tag{2}$$

where E_S and I_S are, respectively, the voltage and current at the sending end of the network and E_R and I_R are, respectively, the voltage and current at the receiving end of the network with the assumed voltage polarities and current directions.

The A, B, C, D parameters can be found from the image impedances and the image-transfer constant of the network. These quantities, namely, the image impedances and the image-transfer constant, can in turn be found merely from open- and short-circuit impedance measurements taken at both the sending and receiving ends of the network. The following equations were used to determine the A, B, C, D constants from open- and short-circuit measurements of each component:

Z_{OC1} = open-circuit impedance looking into end 1 with end 2 open-circuited.

Z_{SC1} = short-circuit impedance looking into end 1 with end 2 short-circuited.

Z_{OC2} = open-circuit impedance looking into end 2 with end 1 open-circuited.

Z_{SC2} = short-circuit impedance looking into end 2 with end 1 short-circuited.

Z_{I1} = image impedance looking into end 1.

Z_{I2} = image impedance looking into end 2.

θ = image-transfer constant.

$$Z_{I1} = \sqrt{Z_{OC1}\, Z_{SC1}} \tag{3}$$

$$Z_{I2} = \sqrt{Z_{OC2}\, Z_{SC2}} \tag{4}$$

$$\theta = \tanh^{-1} \sqrt{\frac{Z_{SC1}}{Z_{OC1}}} = \frac{1}{2} \ln \left[\frac{1 + \sqrt{\dfrac{Z_{SC1}}{Z_{OC1}}}}{1 - \sqrt{\dfrac{Z_{SC1}}{Z_{OC1}}}} \right] \tag{5}$$

$$A = \sqrt{\frac{Z_{I1}}{Z_{I2}}} \cosh\theta \tag{6}$$

$$D = \sqrt{\frac{Z_{I2}}{Z_{I1}}} \cosh\theta \tag{7}$$

$$B = \sqrt{Z_{I1}\, Z_{I2}} \sinh\theta \tag{8}$$

$$C = \frac{\sinh\theta}{\sqrt{Z_{I1}\, Z_{I2}}} \tag{9}$$

The following steps necessary to determine the A, B, C, d parameters are listed in summary:

1) Determine experimentally the open- and short-circuit impedances looking into both ends of the network.

2) Calculate the image impedances from Eqs. (3) and (4) and the image transfer constant from Eq. (5).

3) Then calculate the A, B, C, D parameters from Eqs. (6), (7), (8), and (9).

After the above has been done, we can determine the transmission loss caused by each component of the transmission system from the equation:

$$\text{Transmission loss} = 10 \log_{10} \frac{\mathrm{Re}(E_S \bar{I}_S)}{\mathrm{Re}(E_R \bar{I}_R)} \quad \text{(in db)} \qquad (10)$$

where Re(____) indicates the real part of the quantity within the parentheses and $\bar{I}$ equals the conjugate value of the complex current.

To apply the above theory to the system shown in Fig. 11 after the receiver impedance has been measured and the A, B, C, D constants for each component calculated, a voltage, E_1 is first assumed. Then, knowing Z_R, we can calculate I_1. From the A, B, C, D parameters E_2 and I_2 can be found. Equation (10) is then applied to find the transmission loss caused by the transmission line-RF switch combination, and so on until the antenna terminals are reached.

The transmission lines between the signal goniometer and base-loading resistors and the resistors themselves deserve special mention. Essentially they are in themselves unbalanced devices. However, the two transmission lines will be considered together as being one balanced component; likewise, the resistors at the base of the north and south antennas will be lumped together for the purposes of analysis and will be considered as being one balanced component. If we know the A, B, C, D constants of an unbalanced device, we can calculate the constants, A_t, B_t, C_t, D_t, of two of these unbalanced devices connected in a balanced configuration. Indeed, it can be shown that $A_t = A$, $B_t = 2B$, $C_t = \frac{C}{2}$, and $D_t = D$.

A word should be said about measuring balanced impedances with respect to ground with an unbalanced radio-frequency impedance bridge. A two-wire transmission line can be represented as in Fig. 13. Since $Z_1 = Z_2$ in the balanced case, only two different impedance measurements need be made to determine Z_1 and Z_3. From these measurements we can calculate the

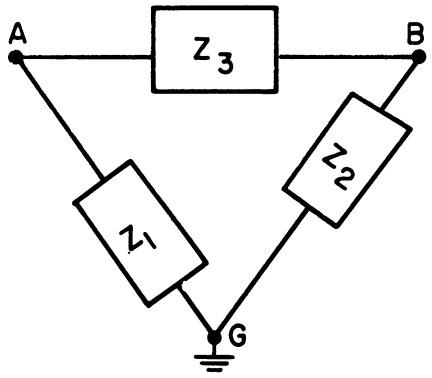

FIG. 13 EQUIVALENT CIRCUIT OF TWO-WIRE TRANSMISSION LINE.

equivalent balanced impedance from A to B. This equivalent balanced impedance was the one used above in all the mentioned calculations. First, A is shorted to B and the impedance measured from this point to ground, G; call this impedance Z_{AB-G}. Next, short B to ground, G, and measure the impedance from A to ground; call this impedance Z_{A-BG}. It can be shown that the impedance between A and B, $Z_{A-B} = \frac{(Z_{AB-G})\ (Z_{A-BG})}{Z_{AB-G} - \frac{1}{4}Z_{A-BG}}$

Clearly, the determination of the transmission loss of each component in the input system is a long and laborious process, but it has some rewards. By knowing the A, B, C, D constants of each component, we can calculate how the component will behave when placed in an entirely different system. Also, two devices designed to perform the same function can be compared by knowing the constants of each. The constants calculated above for each component are tabulated below under the appropriate headings, and the transmission loss calculations are summarized by the graph of Fig. 14 for the low-frequency range from 1.00 to 10.0 megacycles.

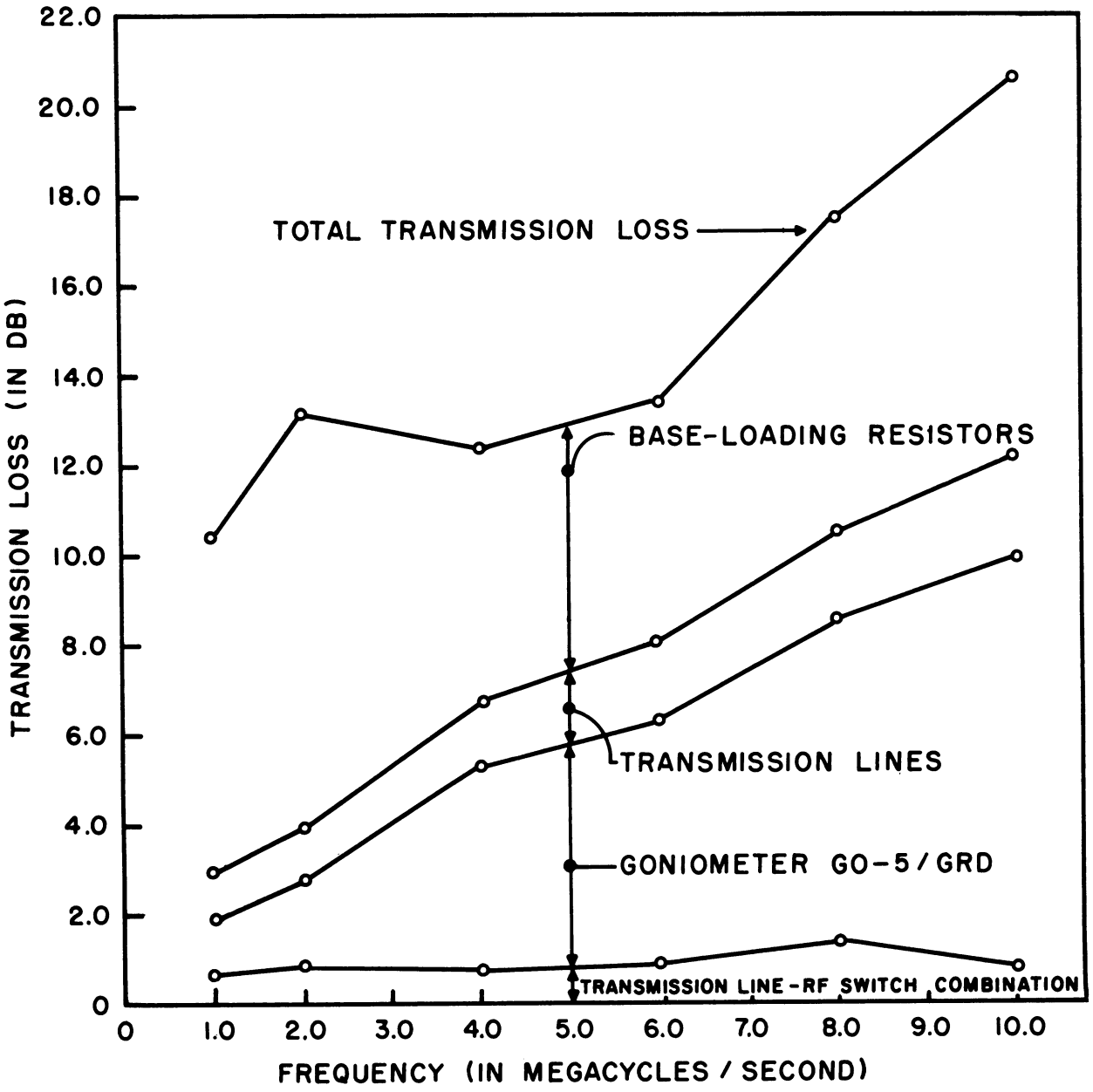

FIG. 14 SUMMARY OF TRANSMISSION LOSS CALCULATIONS— TRANSMISSION LOSS VS. FREQUENCY

5. BASE-LOADING RESISTORS

The base-loading resistors were assumed to be resistive throughout the frequency range used. The A, B, C, D constants are:

$$A_t = 1.4, \quad B_t = 400, \quad C_t = 1 \times 10^{-3}, \quad D_t = 1$$

The contribution of the base-loading resistors to transmission loss as a function of frequency is given in Table I and shown graphically in Fig. 15.

TABLE I

TRANSMISSION LOSS AS A FUNCTION OF FREQUENCY

Frequency (megacycles)	Transmission loss (db)
1.0	7.44
2.0	9.27
4.0	5.70
6.0	5.37
8.0	6.99
10.0	8.39

6. TRANSMISSION LINES

The A, B, C, D parameters for the transmission lines and their transmission loss as a function of frequency are given in Table II. A curve of transmission loss vs frequency for these transmission lines is shown in Fig. 16.

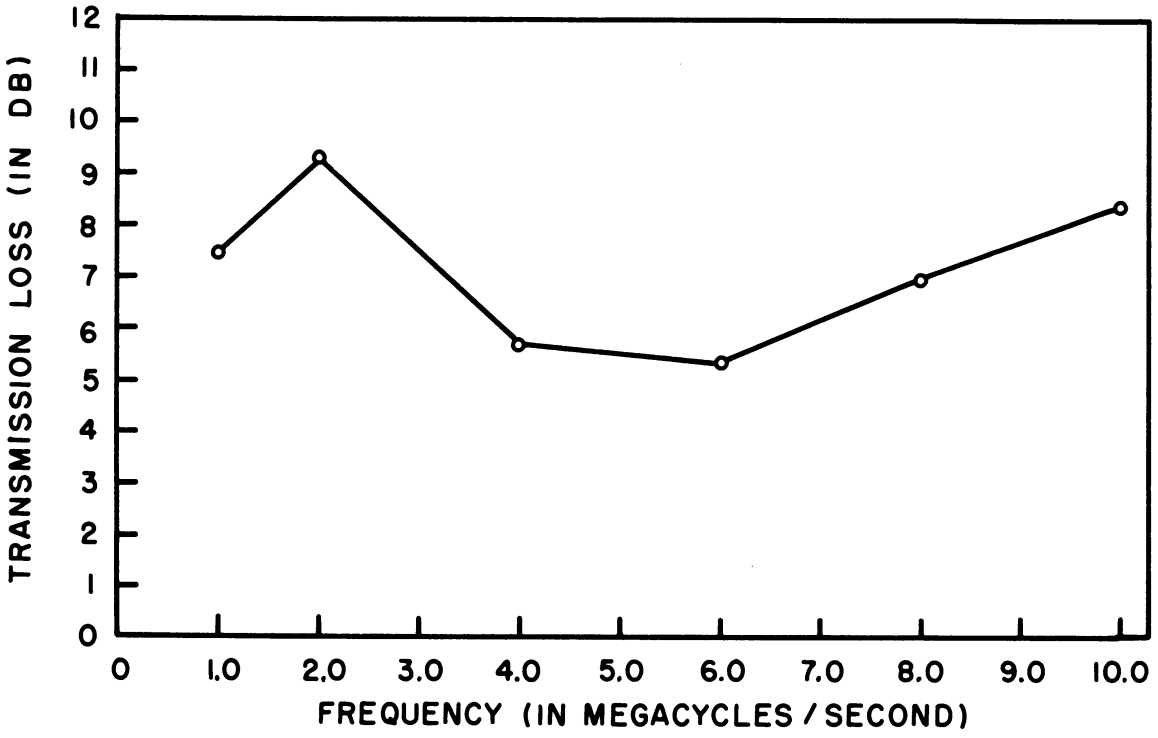

FIG.15 BASE-LOADING RESISTORS-
TRANSMISSION LOSS VS. FREQUENCY

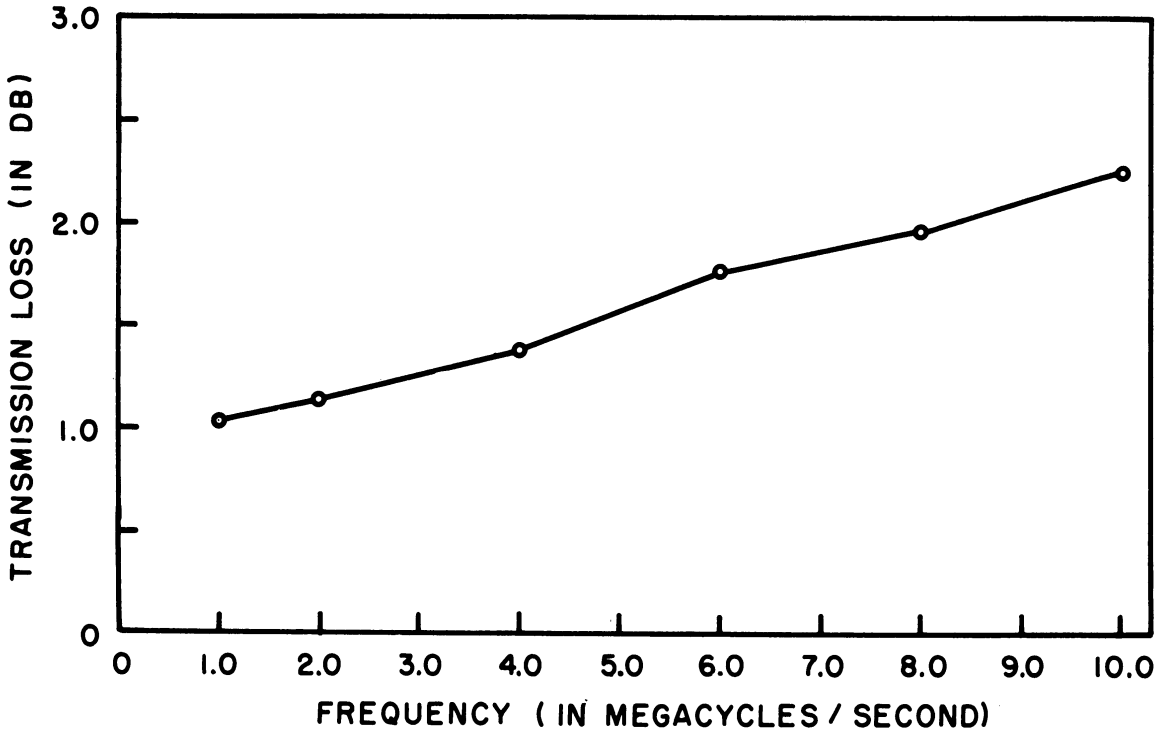

FIG.16 TRANSMISSION LINES-
TRANSMISSION LOSS VS. FREQUENCY

TABLE II

A, B, C, D PARAMETERS AND TRANSMISSION LOSS
AS A FUNCTION OF FREQUENCY (TRANSMISSION LINES)

f	Transmission loss (db)	$A_t = D_t$	B_t	C_t
1.0	1.044	0.0938 /158.2°	147.6 / 90.2°	6.74 x 10^{-3} /90.2°
2.0	1.146	0.985 /180.5°	27.8 /254.5°	1.27 x 10^{-3} /254.5°
4.0	1.394	0.938 / 1.59°	54.0 / 79.2°	2.465 x 10^{-3} / 79.2°
6.0	1.761	0.859 /183.2°	78.0 /261.5°	3.47 x 10^{-3} /261.5°
8.0	1.967	0.759 / 5.2°	98.4 / 83.2°	4.49 x 10^{-3} / 83.2°
10.0	2.25	0.648 /188.0°	114.8 /264.5°	5.245 x 10^{-3} /264.5°

7. ELECTRICAL GONIOMETER GO-5/GRD, Ser. No. 179

The A, B, C, D constants and the transmission loss of the goniometer as a function of frequency are given in Table III. A curve of transmission loss vs frequency is shown in Fig. 17.

TABLE III

A, B, C, D CONSTANTS AND TRANSMISSION LOSS
AS A FUNCTION OF FREQUENCY (GONIOMETER)

f	Transmission loss (db)	A	B	C	D
1.0	1.277	2.58 /-1.20°	87.5/86.60°	43.3 x10^{-3}/-85.64°	1.861/ 1.96°
2.0	1.872	2.51 /-0.39°	169 /87.96°	20.54 x10^{-3}/-82.12°	1.775/ 4.93°
4.0	4.55	2.49 /-4.65°	317 /82.56°	9.27 x10^{-3}/-76.94°	1.580/ 8.85°
6.0	5.37	2.24 / 0.71°	461 /89.1 °	5.02 x10^{-3}/-60.9 °	1.441/19.01°
8.0	7.14	1.974/ 0.55°	574 /88.4 °	2.87 x10^{-1}/-39.2 °	1.228/30.45°
10.0	9.15	1.620/ 1.45°	732 /88.1 °	1.809x10^{-3}/- 3.70°	1.069/47.95°

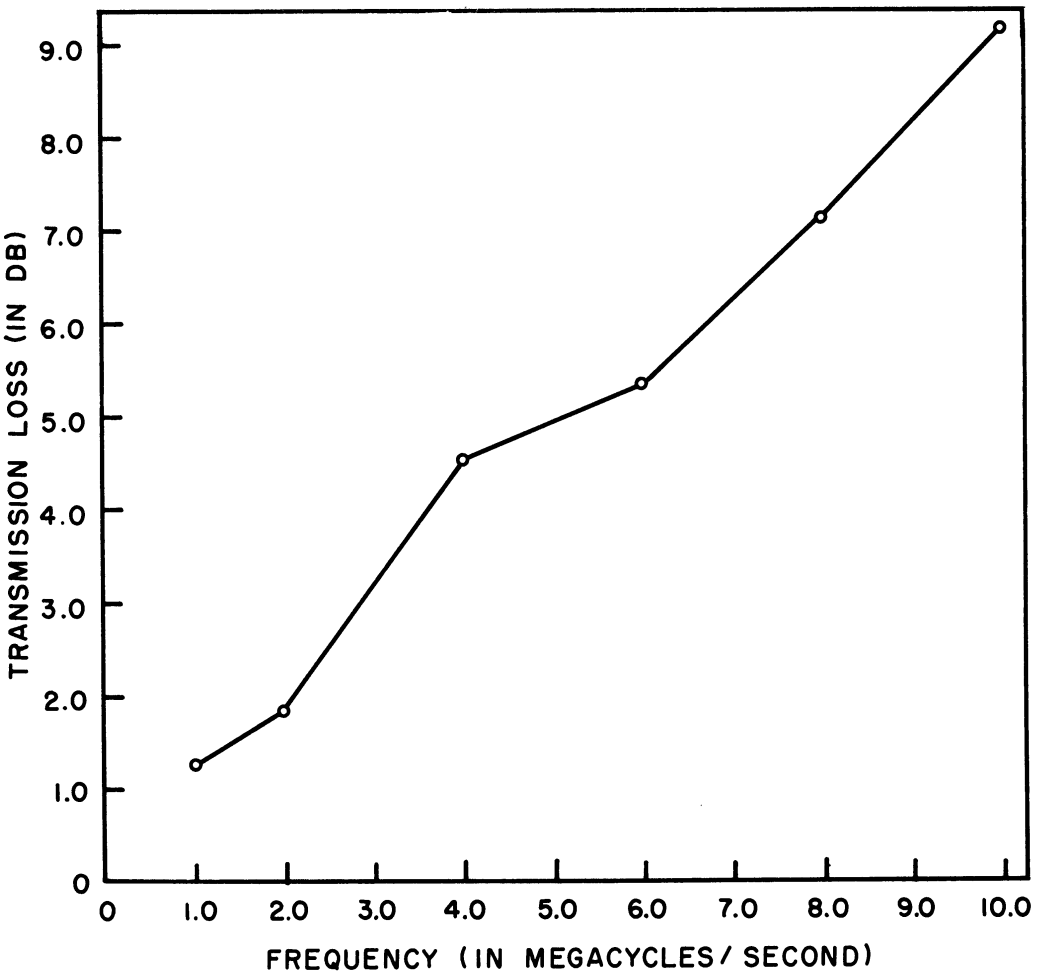

FIG. 17 ELECTRICAL GONIOMETER GO-5/GRD, SER. 179- TRANSMISSION LOSS VS. FREQUENCY

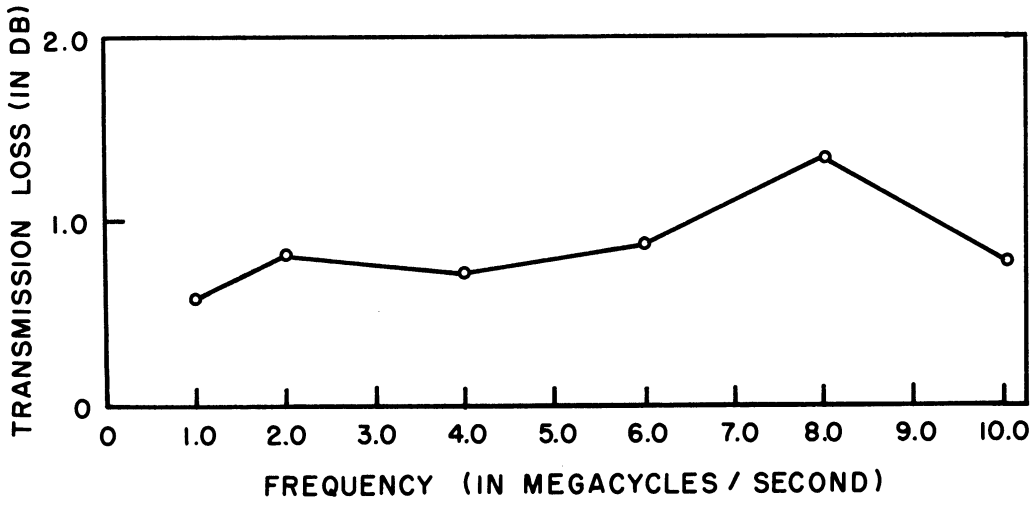

FIG. 18 TRANSMISSION LINE–RF SWITCH COMBINATION– TRANSMISSION LOSS VS. FREQUENCY

8. TRANSMISSION LINE-RF SWITCH COMBINATION

The A, B, C, D parameters and the transmission loss of the line-switch combination as a function of frequency are given in Table IV. A curve of transmission loss vs frequency is shown in Fig 18.

TABLE IV

A, B, C, D PARAMETERS AND TRANSMISSION LOSS AS A FUNCTION OF FREQUENCY (LINE-SWITCH COMBINATION)

f	Transmission loss (db)	A	B	C	D
1.0	0.587	$1.001 \angle 0.13^\circ$	$5.53 \angle 84.61^\circ$	$1.588 \times 10^{-3} \angle 22.59^\circ$	$0.999 \angle 0.35^\circ$
2.0	0.814	$0.993 \angle 0.47^\circ$	$12.39 \angle 86.69^\circ$	$1.892 \times 10^{-3} \angle 38.65^\circ$	$0.995 \angle 0.63^\circ$
4.0	0.715	$0.972 \angle 0.81^\circ$	$25.7 \angle 88.18^\circ$	$2.79 \times 10^{-3} \angle 59.22^\circ$	$0.970 \angle 1.57^\circ$
6.0	0.870	$0.931 \angle 0.48^\circ$	$37.75 \angle 89.38^\circ$	$3.785 \times 10^{-3} \angle 66.76^\circ$	$0.936 \angle 3.32^\circ$
8.0	1.337	$0.877 \angle 1.70^\circ$	$49.8 \angle 89.87^\circ$	$4.76 \times 10^{-3} \angle 73.45^\circ$	$0.886 \angle 3.40^\circ$
10.0	0.779	$0.801 \angle 2.29^\circ$	$61.1 \angle 90^\circ$	$5.71 \times 10^{-3} \angle 76.95^\circ$	$0.830 \angle 4.25^\circ$

9. RECEIVER INPUT IMPEDANCE

The receiver input impedance was measured in the following way. First the entire DF system was connected as it would normally be used and a test signal was transmitted at the proper frequency. The receiver was then tuned to the test frequency, the antenna trim control adjusted for maximum output as indicated on the carrier level meter, and the RF gain control was set to position 8. Impedance measurements were then made at the input to the transmission line-RF switch combination with the receiver connected. At the time of taking these measurements the input signal level

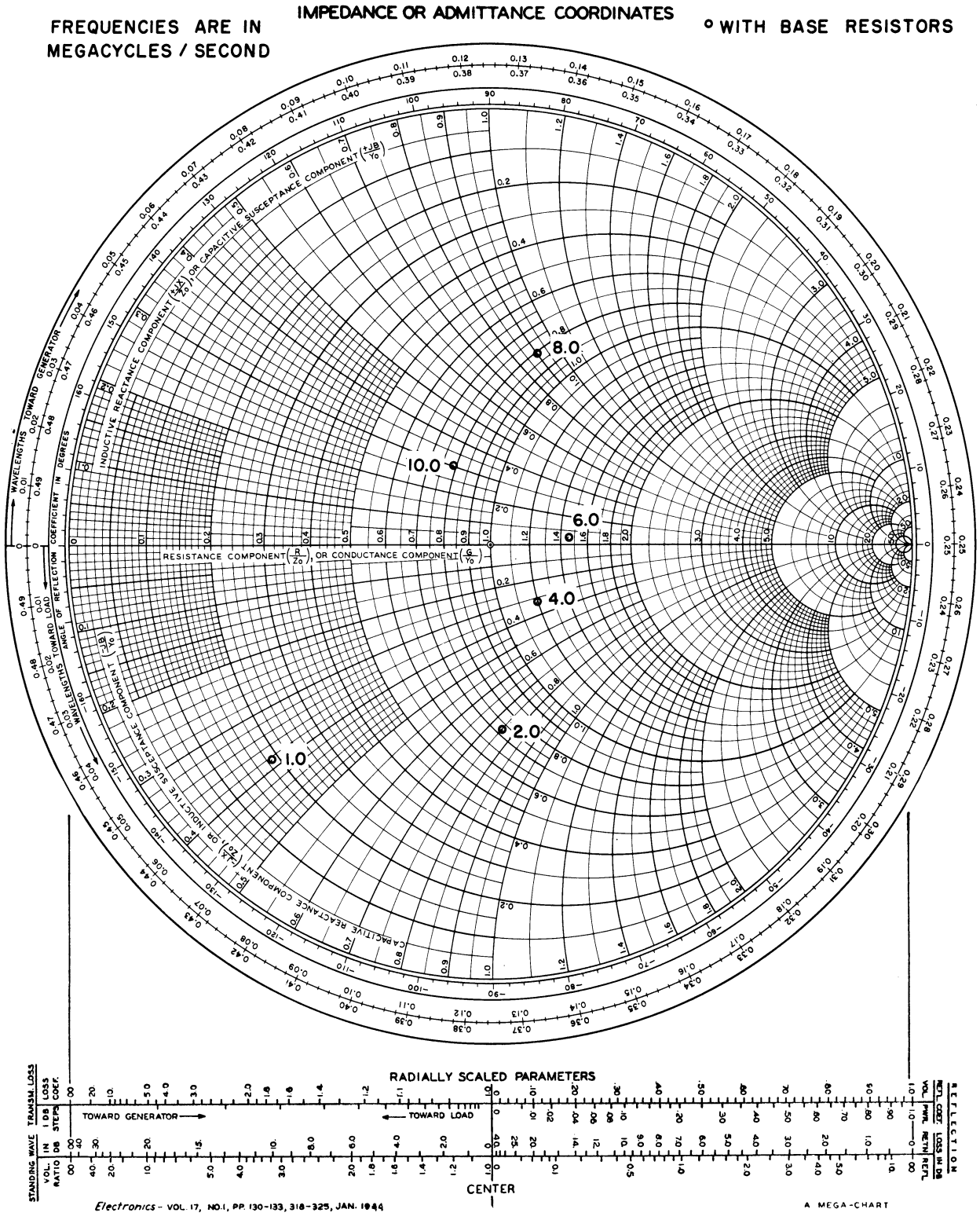

FIG.19 INPUT IMPEDANCE OF RADIO RECEIVER R-390/URR

to the RF bridge was adjusted until a reference voltmeter connected to the plate of the AGC amplifier tube V509 read 15 volts or below for each impedance measurement.

Since all the characteristics of the transmission line-RF switch combination were known, it was a simple calculation to find the actual input impedance of the receiver. The results are tabulated below as a function of frequency and shown graphically in Fig. 19.

TABLE V

RECEIVER INPUT IMPEDANCE AS A FUNCTION OF FREQUENCY

f	Z_R
1.0	18.25 - j36.4
2.0	68.7 - j71.4
4.0	113.2 - j32.2
6.0	139.6 + j 5.61
8.0	77.1 + j85.4
10.0	75.1 + j28.3

10. SUMMARY AND CONCLUSIONS

As a summary of the transmission loss calculations, Fig. 14 was plotted. This shows the cumulative transmission loss as a function of frequency and shows graphically the relative effects of the various components. Clearly, the base-loading resistors are the largest contributing factor to the overall transmission loss. Another observation that can be made is that if care were taken to match the impedance levels the overall transmission loss could be decreased significantly.

DISTRIBUTION LIST

Copy No.	
1-2	Commanding Officer, U. S. Army Signal Research and Development Laboratory, Fort Monmouth, New Jersey, ATTN: Senior Scientist, Countermeasures Division
3	Commanding General, U. S. Army Electronic Proving Ground, Fort Huachuca, Arizona, ATTN: Director, Electronic Warfare Department
4	Chief, Research and Development Division, Office of the Chief Signal Officer, Department of the Army, Washington 25, D. C., ATTN: SIGEB
5	Chief, Plans and Operations Division, Office of the Chief Signal Officer, Washington 25, D. C., ATTN: SIGEW
6	Commanding Officer, Signal Corps Electronics Research Unit, 9560th USASRU, P. O. Box 205, Mountain View, California
7	U. S. Atomic Energy Commission, 1901 Constitution Avenue, N.W., Washington 25, D. C., ATTN: Chief Librarian
8	Director, Central Intelligence Agency, 2430 E Street, N.W., Washington 25, D. C., ATTN: OCD
9	Signal Corps Liaison Officer, Lincoln Laboratory, Box 73, Lexington 73, Massachusetts, ATTN: Col. Clinton W. Janes
10-19	Commander, Armed Services Technical Information Agency, Arlington Hall Station, Arlington 12, Virginia
20	Commander, Air Research and Development Command, Andrews Air Force Base, Washington 25, D. C., ATTN: RDTC
21	Directorate of Research and Development, USAF, Washington 25, D. C., ATTN: Chief, Electronic Division
22-23	Commander, Wright Air Development Center, Wright Patterson Air Force Base, Ohio, ATTN: WCOSI-3
24	Commander, Wright Air Development Center, Wright-Patterson Air Force Base, Ohio, ATTN: WCLGL-7
25	Commander, Air Force Cambridge Research Center, L. G. Hanscom Field, Bedford, Massachusetts, ATTN: CROTLR-2
26	Commander, Rome Air Development Center, Griffiss Air Force Base, New York, ATTN: RCSSLD
27	Commander, Air Proving Ground Center, ATTN: Adj/Technical Report Branch, Eglin Air Force Base, Florida
28	Commander, Special Weapons Center, Kirtland Air Force Base, Albuquerque, New Mexico
29	Chief, Bureau of Ordnance, Code ReO-1, Department of the Navy, Washington 25, D. C.
30	Chief of Naval Operations, EW Systems Branch, OP-347, Department of the Navy Washington 25, D. C.
31	Chief, Bureau of Ships, Code 840, Department of the Navy, Washington 25, D. C.
32	Chief, Bureau of Ships, Code 843, Department of the Navy, Washington 25, D. C.
33	Chief, Bureau of Aeronautics, Code EL-8, Department of the Navy, Washington 25, D. C.
34	Commander, Naval Ordnance Test Station, Inyokern, China Lake, California, ATTN: Test Director-Code 30
35	Commander, Naval Air Missile Test Center, Point Mugu, California, ATTN: Code 366
36	Director, Naval Research Laboratory, Countermeasures Branch, Code 5430, Washington 25, D. C.
37	Director, Naval Research Laboratory, Washington 25, D. C., ATTN: Code 2021
38	Director, Air University Library, Maxwell Air Force Base, Alabama, ATTN: CR-4987
39	Commanding Officer-Director, U. S. Naval Electronic Laboratory, San Diego 52, California
40	Office of the Chief of Ordnance, Department of the Army, Washington 25, D. C., ATTN: ORDTU
41	Chief, West Coast Office, U. S. Army Signal Research and Development Laboratory, Bldg. 6, 75 S. Grand Avenue, Pasadena 2, California
42	Commanding Officer, U. S. Naval Ordnance Laboratory, Silver Springs 19, Maryland
43-44	Chief, U. S. Army Security Agency, Arlington Hall Station, Arlington 12, Virginia, ATTN: GAS-24L

DISTRIBUTION LIST (Cont'd)

Copy No.	
45	President, U. S. Army Defense Board, Headquarters, Fort Bliss, Texas
46	President, U. S. Army Airborne and Electronics Board, Fort Bragg, North Carolina
47	U. S. Army Antiaircraft Artillery and Guided Missile School, Fort Bliss, Texas, ATTN: E & E Department
48	Commander, USAF Security Service, San Antonio, Texas, ATTN: CLR
49	Chief of Naval Research, Department of the Navy, Washington 25, D. C., ATTN: Code 931
50	Commanding Officer, U. S. Army Security Agency, Operations Center, Fort Huachuca, Arizona
51	President, U. S. Army Security Agency Board, Arlington Hall Station, Arlington, 12, Virginia
52	Operations Research Office, Johns Hopkins University, 6935 Arlington Road, Bethesda 14, Maryland, ATTN: U. S. Army Liaison Officer
53	The Johns Hopkins University, Radiation Laboratory, 1315 St. Paul Street, Baltimore 2, Maryland, ATTN: Librarian
54	Stanford Electronics Laboratories, Stanford University, Stanford, California, ATTN: Applied Electronics Laboratory Document Library
55	HRB-Singer, Inc., Science Park, State College, Penn., ATTN: R. A. Evans, Manager, Technical Information Center
56	ITT Laboratories, 500 Washington Avenue, Nutley 10, New Jersey, ATTN: Mr. L. A. DeRosa, Div. R-15 Lab.
57	The Rand Corporation, 1700 Main Street, Santa Monica, California, ATTN: Dr. J. L. Hult
58	Stanford Electronics Laboratories, Stanford University, Stanford, California, ATTN: Dr. R. C. Cumming
59	Willow Run Laboratories, The University of Michigan, P. O. Box 2008, Ann Arbor Michigan, ATTN: Dr. Boyd
60	Stanford Research Institute, Menlo Park, California, ATTN: Dr. Cohn

Copy No.	
61-62	Commanding Officer, U. S. Army Signal Missile Support Agency, White Sands Missile Range, New Mexico, ATTN: SIGWS-EW and SIGWS-FC
63	Commanding Officer, U. S. Naval Air Development Center, Johnsville, Pennsylvania, ATTN: Naval Air Development Center Library
64	Commanding Officer, U. S. Army Signal Research and Development Laboratory, Fort Monmouth, New Jersey, ATTN: U. S. Marine Corps Liaison Office, Code AO-4C
65	President U. S. Army Signal Board, Fort Monmouth, New Jersey
66-76	Commanding Officer, U. S. Army Signal Research and Development Laboratory, Fort Monmouth, New Jersey ATTN: 1 Copy - Direcotr of Research 1 Copy - Technical Documents Center ADT/E 1 Copy - Chief, Ctms Systems Branch, Countermeasures Division 1 Copy - Chief, Detection & Location Branch, Countermeasures Division 1 Copy - Chief, Jamming & Deception Branch, Countermeasures Division 1 Copy - File Unit No. 4, Mail & Records, Countermeasures Division 1 Copy - Chief, Vulnerability Br., Electromagnetic Environment Division 1 Copy - Reports Distribution Unit, Countermeasures Division File 3 Cpys - Chief, Security Division (for retransmittal to BJSM)
77	Director, National Security Agency, Ft. George G. Meade, Maryland, ATTN: TEC
78	Dr. H. W. Farris, Director, Cooley Electronics Laboratory, University of Michigan Research Institute, Ann Arbor, Michigan
79-99	Cooley Electronics Laboratory Project File, University of Michigan Research Institute, Ann Arbor, Michigan
100	Project File, University of Michigan Research Institute, Ann Arbor, Michigan

Above distribution is effected by Countermeasures Division, Surveillance Dept., USASRDL, Evans Area, Belmar, New Jersey. For further information contact Mr. I. O. Myers, Senior Scientist, telephone PRospect 5-3000, Ext. 61252.